Theory of Double-Chirped Mirrors

Nicolai Matuschek, Franz X. Kärtner, and Ursula Keller, *Member, IEEE*

***Abstract*— A theory of double-chirped mirrors (DCM's) for dispersion compensation in ultrashort pulse laser sources is presented. We describe the multilayer interference coating by exact coupled-mode equations. They show that the analysis and synthesis of a coating with a slowly varying chirp in the layer thicknesses can be mapped onto a weakly inhomogeneous transmission line problem. Solutions of the transmission line equations are given using the WKB-method. Analytic expressions for reflectivity and group delay are derived. The solutions show that the main problem in chirped mirror design is the avoidance of spurious reflections, that lead to Gires–Tournois-like interference effects responsible for the oscillations in the group delay. These oscillations are due to an impedance matching problem of the equivalent transmission line. The impedance matching can be achieved by simultaneously chirping the strength of the coupling coefficient and the Bragg wavenumber of the mirror. An adiabatic increase in the coupling coefficient removes the typical oscillations in the group delay and results in broad-band mirrors with a controlled dispersion. Finally, the mirror is matched to air with a broadband antireflection coating. We discuss a complete design of a laser mirror with a reflectivity larger than 99.8% and a controlled dispersion over 400-nm bandwidth. Using such mirrors in a Ti:sapphire laser, we have demonstrated ≈30-fs pulses, tunable over 300 nm, as well as 8-fs pulses from the same setup. A different design resulted in 6.5-fs pulses.**

***Index Terms*—Chirped mirrors, coatings, coupled-mode analysis, dielectric films, electromagnetic coupling, thin-film devices, transmission line theory, WKB analysis.**

I. Introduction

ULTRASHORT pulse generation has advanced to a level where the bandwidth of standard Bragg mirrors, composed of SiO_2 and TiO_2 quarter-wave layers, limits the pulse width [Fig. 1(a)]. The limitation is two fold. First, due to the limited difference in refractive index of both materials, $n_{SiO_2} \approx 1.45$ and $n_{TiO_2} \approx 2.4$, the high-reflectivity bandwidth of a standard quarter-wave Bragg mirror at 800 nm is only about 200 nm. Second, the higher order group delay dispersion (GDD) produced by quarter-wave Bragg mirrors further limits the useful bandwidth to about 100 nm for 10-fs pulses. The effects of the dispersion from quarter-wave Bragg mirrors on short pulse generation has already been investigated with CPM-dye lasers ([1], and references therein).

In a chirped mirror, the Bragg wavelength λ_B of the individual layer pairs is varied from layer pair to layer pair (e.g., linearly), so that longer wavelengths penetrate deeper into the mirror structure than shorter wavelengths before being reflected [Fig. 1(b)]. Such mirrors show an enlarged high-reflectivity range. However, the dispersion properties of these mirrors were found to be inadequate for ultrashort pulse generation [2]. Szipöcs and Krausz designed the first chirped mirrors with an extended high-reflectivity range and a controlled group delay [3], [4]. For 10 fs-Ti:sapphire lasers, multiple bounces on such mirrors achieve enough negative GDD to compensate for the positive dispersion in the laser crystal, without any additional use of prism pairs [5]. Even fused quartz prism pairs generate too much higher order dispersion for sub-10-fs pulse generation [6]. Chirped mirrors are also beneficial for the compression of high energy pulses, because they produce high dispersion with little material in the beam path, thereby avoiding nonlinear effects in the compressor [7]. Thus, the design of these mirrors is extremely important for the further development of ultrafast laser physics.

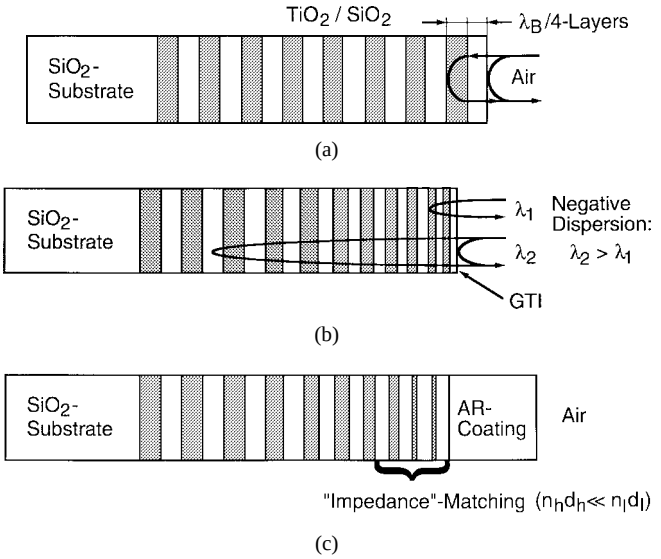

Fig. 1. Schematic of different types of mirrors. (a) Standard dielectric quarter-wave Bragg mirror. (b) Simple-chirped mirror. Here, the Bragg wavelength is chirped to higher values, such that longer wavelengths penetrate deeper into the mirror than shorter wavelengths, producing a negative GDD. (c) DCM. An impedance-matching section and an AR-coating on top of the mirror avoid the oscillation in the group delay.

It turns out that the simple picture of a chirped mirror, as presented in Fig. 1(b), is not true. Using standard transfer matrix analysis of the multilayer structure, one observes that the group delay produced by such a chirped mirror does not vary linearly with wavelength, as one would expect for a mirror with linearly chirped Bragg wavelength. The average of the group delay shows the expected tendency to increase linearly with increasing wavelength. However, it also exhibits strong oscillations (Fig. 2, dotted lines) [2].

Manuscript received October 10, 1997; revised March 2, 1998. This work was supported by the Swiss National Science Foundation.

The authors are with the Swiss Federal Institute of Technology, Zurich (ETH), Institute of Quantum Electronics, Ultrafast Laser Physics Laboratory, CH-8093 Zurich, Switzerland.

Publisher Item Identifier S 1077-260X(98)03766-6.

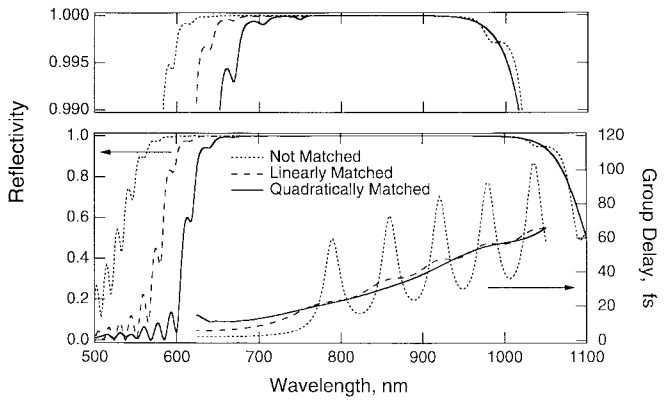

Fig. 2. Reflectivity and group delay for a mirror which is linearly chirped in the Bragg wavenumber, as described in Fig. 6. The upper plot shows an enlarged view of the top 1% of the reflectivity. The dotted lines show the results for a simple-chirped mirror (i.e., impedance is not matched). The dashed and solid lines show results for a DCM, where both the Bragg wavenumber and the thickness of the high-index layers are chirped. The dashed and solid lines represent the case of linearly and quadratically chirped high-index layers, respectively, as described in Fig. 7.

The cause of these oscillations is the following. Longer wavelengths have to pass the first section of the Bragg mirror, which acts as a transmission grating for these wavelengths. Slight reflections in the front section interfere with the strong reflection from the back, as in a Gires–Tournois interferometer (GTI) [8]. The oscillations in the group delay have an amplitude of several tens of femtoseconds, which make these simple-chirped mirrors useless for ultrashort pulse generation. Szipöcs and others eliminate these oscillations by using special computer optimization algorithms [3]. Recently, a semi-empirical algorithm has been presented that results in a starting structure for computer optimization [9]. In the case of chirped Bragg gratings, the oscillations are suppressed by apodization of the grating [10], [11], i.e., an adiabatic increase or decrease of the coupling in the reflected wave at the beginning and end of the grating.

The transfer matrix calculus usually used to evaluate dielectric multilayer coatings is easy to implement, but it gives very little insight into how a chirped mirror works and it does not answer the following questions. What kind of starting structure is appropriate for computer optimization, in order to achieve a certain group delay? How much negative second, third or higher order dispersion can be produced with a mirror composed of two given materials? To answer at least some of these questions analytic insight is needed. Recently, we have shown that coupled-mode theory, originally invented to describe the interaction of beams propagating in weakly index modulated media, is structurally equivalent to the transfer matrix method for layered media composed of two different materials [12]. In this paper, we use these results to derive a detailed theory for chirped mirrors, which results in double-chirped mirrors (DCM's), as briefly described in [13]. Fig. 2 (dashed and solid lines) summarizes the effects of double chirping. We can clearly see that, in principle, it is possible to reduce and eliminate the disturbing oscillation in the group delay by a sufficiently slow increase in the coupling coefficient in the front section of the mirror. This comes at the expense of some of the bandwidth of the high-reflectivity region, as will be explained later.

The paper is organized as follows. In Section II, we state the main results of [12] and clarify notation. A dielectric multilayer structure can be thought of as a strongly inhomogeneous transmission line. The introduction of coupled-mode equations transforms the strongly inhomogenous transmission line into a transmission line with a slowly varying characteristic impedance, as described in Section III. The transmission line model for the chirped Bragg grating gives two stationary Schrödinger equations for the equivalent voltage and current. In Section IV, we study the solutions of these Schrödinger equations qualitatively using WKB-solutions and derive an explicit expression for the complex reflection coefficient of the mirror. The expression shows that the origin of the oscillation in the group delay is an impedance mismatch in the front section of the mirror. This impedance mismatch and, therefore, the oscillation in the group delay, can be eliminated, if we chirp the coupling coefficient along with the period of the grating [Fig. 1(c) and Fig. 2, dashed and solid lines]. In this way, we generate DCM's with a controlled group delay and an extended high-reflectivity range in comparison with standard dielectric Bragg mirrors. In Section V, we demonstrate the use of the WKB-solutions to generate a starting structure for a mirror with a desired group delay and a desired high-reflectivity range. The analytic starting structure automatically avoids internal resonances in the multilayer structure, which might plague other mirror designs. The second matching problem, the matching of the mirror to the air using a broad-band antireflection (AR)-coating, is discussed in Section VI. Based on these considerations, we have designed a broad-band mirror with a reflectivity higher than 99.8% and a smooth group delay over a bandwidth of almost 400 nm. As we have demonstrated, a set of these mirrors in a Ti:sapphire laser is appropriate for the tunability of ≈30-fs pulses over a bandwidth of 300 nm (700–1000 nm). Additionally, we have used these DCM's in the same setup for the generation of 8-fs pulses [14].

II. Description of Multilayer Interference Coatings with Exact Coupled-Mode Equations

A multilayer coating is composed of alternating layers with high and low refractive indices, $n_{\rm h}$ and $n_{\rm l}$, respectively (Fig. 3). In a standard quarter-wave Bragg mirror, the optical thickness of each layer equals a quarter of the center wavelength λ_B in the stopband of the mirror, i.e., $d_{\rm h} \cdot n_{\rm h} = d_{\rm l} \cdot n_{\rm l} = \lambda_B/4$. The analysis of such a mirror by transfer matrix theory or coupled-mode theory and the resulting reflection and transmission properties can be found in standard text books. In the following, we generally call a Bragg mirror with unequal optical properties of the individual index steps a chirped mirror.

The coupled-mode equations for a chirped mirror are [12]

$$\frac{d}{dz}\begin{pmatrix}\tilde{A}(z)\\ \tilde{B}(z)\end{pmatrix} = i\begin{pmatrix}-\beta & -\tilde{\kappa}e^{-i\phi_B}\\ \tilde{\kappa}e^{i\phi_B} & \beta\end{pmatrix}\begin{pmatrix}\tilde{A}(z)\\ \tilde{B}(z)\end{pmatrix}. \quad (1)$$

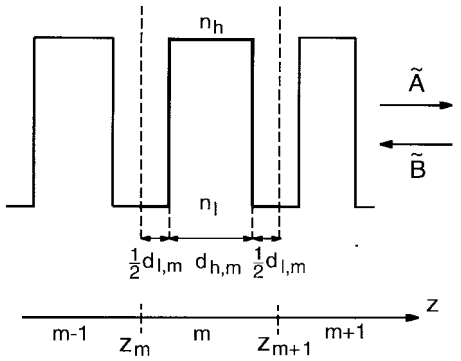

Fig. 3. Refractive-index profile of a chirped mirror with a symmetrically defined local Bragg period.

Here, $\tilde{A}$ and $\tilde{B}$ are the complex amplitudes of the forward and backward propagating wave, respectively, see Fig. 3. The coefficients in the equation are the local effective propagation constant $\beta(z)$, the local coupling coefficient $\tilde{\kappa}(z)$ and the Bragg phase $\phi_B(z)$. To describe a chirped mirror with coupled-mode theory exactly, these coefficients have to be determined for an actual layer structure, according to [12]

$$\beta(z) = \frac{1}{2}\,\frac{d\phi_B(z)}{dz} + \tilde{\delta}(z) \tag{2}$$

where

$$\phi_B(z) = \int_0^z \frac{2\pi}{\Lambda(\overline{z})}\,d\overline{z} \tag{3}$$

$$\tilde{\delta}(z) = -\frac{\alpha}{\Lambda}\,\frac{1}{1-r^2}\,(\sin(\phi) + r^2\sin(\Delta\phi)) \tag{4}$$

and

$$\tilde{\kappa}(z) = -\frac{\alpha}{\Lambda}\,\frac{2r}{1-r^2}\,\sin(\phi_{\mathrm{h}}) \tag{5}$$

with

$$r = \frac{n_{\mathrm{h}} - n_{\mathrm{l}}}{n_{\mathrm{h}} + n_{\mathrm{l}}}. \tag{6}$$

Here, $\tilde{\delta}(z)$ denotes the exact detuning coefficient. The detuning and coupling coefficients are constant within the interval $z \in [z_m, z_{m+1}]$, where $(-m) \in \mathbb{N}$ counts the number of symmetric index steps, see Fig. 3. $\Lambda(z_m) = d_{\mathrm{h,m}} + d_{\mathrm{l,m}}$ is the total length of the $(-m)$th index step, and r is the Fresnel reflectivity at one index discontinuity. In (2)–(5), $\phi_{\mathrm{h/l}} = kn_{\mathrm{h/l}}\,d_{\mathrm{h/l}}$ denote the optical phase shift in the high/low-index layer, $\phi = k(n_{\mathrm{h}}\,d_{\mathrm{h}} + n_{\mathrm{l}}\,d_{\mathrm{l}})$ is the total optical phase shift, and $\Delta\phi = k(n_{\mathrm{h}}\,d_{\mathrm{h}} - n_{\mathrm{l}}\,d_{\mathrm{l}})$ is the difference in the optical phase shifts, where $k = (\omega/c)$ is the vacuum wavenumber.

In the following, we denote

$$k_B = \frac{2\pi}{\lambda_B} = \frac{\pi}{n_{\mathrm{h}}\,d_{\mathrm{h}} + n_{\mathrm{l}}\,d_{\mathrm{l}}} \tag{7}$$

as the Bragg wavenumber, because it is the wavenumber where the strongest Bragg reflection occurs. In contrast to [12], we define the factor α by

$$\alpha = \mathrm{sign}\,(-F_{\mathrm{R}})\,\frac{\eta}{\sinh(\eta)} \tag{8}$$

with

$$\eta = \begin{cases} \ln(|F_{\mathrm{R}}| + \sqrt{F_{\mathrm{R}}^2 - 1}), & \text{for } |F_{\mathrm{R}}| \geqq 1 \\ i\arctan\left(\dfrac{\sqrt{1-F_{\mathrm{R}}^2}}{|F_{\mathrm{R}}|}\right), & \text{for } |F_{\mathrm{R}}| < 1 \end{cases} \tag{9}$$

where

$$F_{\mathrm{R}} = \frac{1}{1-r^2}\,(\cos(\phi) - r^2\cos(\Delta\phi)) \tag{10}$$

in order to avoid complex coupling and detuning coefficients for the case $F_{\mathrm{R}} > +1$. This situation may arise when the optical thicknesses of the high-and low-index layer are not equal $(\Delta\phi \neq 0)$. With the definition given here, the coupling and detuning coefficients are real quantities for all cases, but they are discontinuous when F_{R} changes from negative to positive values. In addition, for the case $F_{\mathrm{R}} > 0$, the transfer matrix of the chirped Bragg grating resulting from a solution of (1) differs by an overall factor $(-1)^N$ from the correct transfer matrix, where $N \in \mathbb{N}$ is the total number of index steps considered. However, this factor is irrelevant for the computation of the reflectivity and the group delay. Therefore, we skip it.

We introduce the slowly varying field amplitudes with respect to the Bragg phase, i.e.,

$$A = \tilde{A}e^{i\phi_B(z)/2} \tag{11}$$

$$B = \tilde{B}e^{-i\phi_B(z)/2}. \tag{12}$$

The slowly varying amplitudes for the forward and backward waves obey the following coupled-mode equations, normalized with respect to an index step of thickness $\delta m = 1$, i.e., $dz = dm \cdot \Lambda(z)$

$$\frac{d}{dm}\begin{pmatrix} A(m) \\ B(m) \end{pmatrix} = i\begin{pmatrix} -\delta(m) & -\kappa(m) \\ \kappa(m) & \delta(m) \end{pmatrix}\begin{pmatrix} A(m) \\ B(m) \end{pmatrix} \tag{13}$$

where m is now considered to be a continuous variable. $\kappa(m) = \tilde{\kappa}\Lambda$ and $\delta(m) = \tilde{\delta}\Lambda$ are the normalized local coupling and detuning coefficients, respectively, which describe the multilayer coating completely.

These coefficients are functions of only two independent variables, for example ϕ and $\Delta\phi$, according to (4) and (5). Fig. 4(a) and (b) show plots of both coefficients as a function of ϕ and $\Delta\phi$. In this paper, we are interested in a correct description of broad-band highly reflecting laser mirrors. Thus, we will always operate at wavelengths where $\phi \approx \pi$. Fig. 4 shows that a linearization of the coefficients around π with respect to ϕ gives an excellent approximation over the range $|\phi - \pi| \leqq \pi/2$, if the expansion coefficients are considered to be functions of $\Delta\phi$. For a chirped mirror composed of TiO_2/SiO_2, the Fresnel reflectivity r is approximately 0.25. Since r is small, we can even neglect quadratic or higher order terms in r. Then $F_{\mathrm{R}}(\phi = \pi) = -1$ and $\alpha(\phi = \pi) = 1$ and we obtain

$$\kappa(\phi, \Delta\phi) = -2r\left\{\cos\left(\frac{\Delta\phi}{2}\right) - \frac{1}{2}\,\sin\left(\frac{\Delta\phi}{2}\right)(\phi - \pi)\right\} \tag{14}$$

$$\delta(\phi, \Delta\phi) = \phi - \pi = \pi\left(\frac{k}{k_B} - 1\right). \tag{15}$$

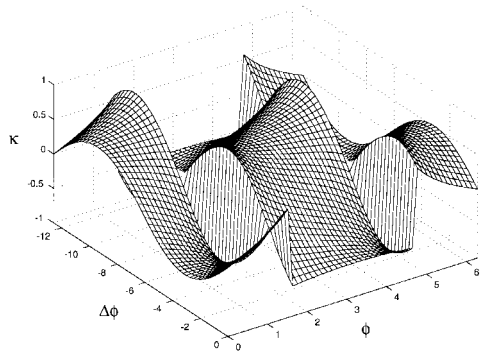

(a)

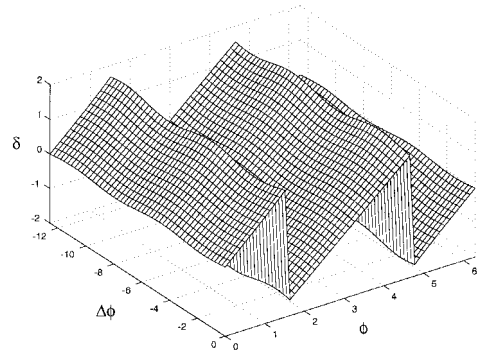

(b)

Fig. 4. (a) Exact coupling coefficient and (b) exact detuning coefficient as functions of ϕ and $\Delta\phi$, which are the sum and difference phase shifts in the high- and low-index layers. The coupling coefficient depends on both ϕ and $\Delta\phi$, whereas the detuning coefficient depends almost only on ϕ.

As we can see, the detuning coefficient depends only on ϕ. In contrast, the coupling coefficient depends on both, ϕ and $\Delta\phi$. Thus, the coupling and detuning coefficients can be engineered independently.

III. Equivalent Transmission Line Model

A multilayer coating can also be considered as a strongly inhomogeneous microwave transmission line, with variations on a subwavelength scale. If the coupling and detuning coefficients vary slowly from index step to index step, the coupled-mode equations for the slowly varying amplitudes (13) do not show this strong inhomogeneity. Thus, we can go backward from the coupled-mode equations to weakly inhomogeneous transmission line equations.

We introduce the generalized voltage V and current I of an effective TEM-transmission line (see Fig. 5) [15], [16], equivalent to the forward and backward propagating waves in the modulated medium. With

$$V = \frac{1}{\sqrt{2}}\,(A+B) \tag{16}$$

$$I = \frac{1}{\sqrt{2}}\,(A-B) \tag{17}$$

we obtain from (13)

$$\frac{dV}{dm} = -iX(m)I \tag{18}$$

$$\frac{dI}{dm} = -iY(m)V \tag{19}$$

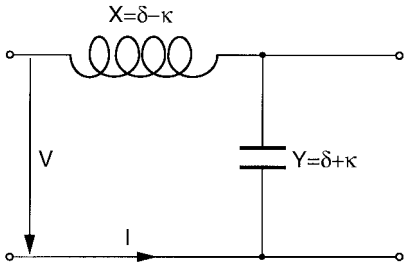

Fig. 5. Equivalent transmission line model for the coupled-mode problem. The reactance X and susceptance Y change slowly along the transmission line.

with the generalized inhomogeneous reactance X and susceptance Y

$$X(m) = \delta(m) - \kappa(m) \tag{20}$$

and

$$Y(m) = \delta(m) + \kappa(m) \tag{21}$$

that depend on the index step considered. If the Bragg grating under consideration consists of identical index steps, the new transmission line is homogeneous, whereas the original problem would be strongly inhomogeneous. Of course, the voltages and currents of the new transmission line only agree with those of the old ones at the discrete values of m. The telegraph equations (18) and (19) can be used to derive two stationary Schrödinger equations for the voltage and current. In order to do so, we assume that the coupling and detuning coefficients are sufficiently smooth functions of m. Thus, we think of a smoothed version of the stepwise constant coupling and detuning coefficient over m.

Elimination of the voltage or current from (18) and (19) leads to

$$\frac{d^2V}{dm^2} - \frac{X'}{X}\,\frac{dV}{dm} + XYV = 0 \tag{22}$$

$$\frac{d^2I}{dm^2} - \frac{Y'}{Y}\,\frac{dI}{dm} + XYI = 0. \tag{23}$$

Here and in the following, a prime at physical quantities denotes their derivative with respect to m. The substitutions

$$V = \sqrt{X}\tilde{V} \quad \text{and} \quad I = \sqrt{Y}\tilde{I} \tag{24}$$

yield

$$-\frac{d^2\tilde{V}}{dm^2} + U_V(m)\tilde{V} = 0 \tag{25}$$

and

$$-\frac{d^2\tilde{I}}{dm^2} + U_I(m)\tilde{I} = 0 \tag{26}$$

with the potentials

$$U_V(m) = U_0(m) + U_{V,1}(m) \tag{27}$$

$$U_I(m) = U_0(m) + U_{I,1}(m) \tag{28}$$

where

$$U_0(m) = -XY = \kappa^2 - \delta^2 \tag{29}$$

$$U_{V,1}(m) = \frac{3}{4}\frac{X'^2}{X^2} - \frac{1}{2}\frac{X''}{X} \tag{30}$$

$$U_{I,1}(m) = \frac{3}{4}\frac{Y'^2}{Y^2} - \frac{1}{2}\frac{Y''}{Y}. \tag{31}$$

Equations (25) and (26) are Schrödinger equations with scattering potentials U_V and U_I. The kinetic energy of the incident "particle" is zero. These Schrödinger equations can be solved by standard methods known from Quantum Mechanics. Here, we are interested in qualitative solutions to understand the origin of the oscillation in the group delay of a mirror with a chirped Bragg wavenumber and how to prevent it.

IV. WKB-Solutions for Mirrors

A. General WKB-Solution for a Mirror

The WKB-method [17] is applicable to our problem if we assume that the scattering potentials $U_{V/I}$ are only slowly varying functions over the index steps, while the wave functions $\tilde{V}$ and $\tilde{I}$ vary on the scale of m. In terms of the coupling and detuning coefficients, this condition is written as $(1/\kappa)(d\kappa/dm) = O(\varepsilon) \ll 1$ and $(1/\delta)(d\delta/dm) = O(\varepsilon) \ll 1$. Then, the additional corrections in the potential (30) and (31) contribute only to second order, as shown in Appendix A. We neglect these terms in the following, because these terms lead to effects one order beyond the usually used and well-known WKB-solution in physical optics approximation [17]. Thus, we are interested in the WKB-solution of

$$-\frac{d^2\tilde{V}}{dm^2} + U_0\tilde{V} = 0 \tag{32}$$

$$-\frac{d^2\tilde{I}}{dm^2} + U_0\tilde{I} = 0. \tag{33}$$

The equations for the current and the voltage are now identical, but one has to remember that they are derived from different equations, where we neglected the term $U_{V,1}$ or $U_{I,1}$, The turning points of the classical motion, corresponding to (32) or (33), are determined by the zeros of the potential

$$U_0 = 0 \Rightarrow \quad X = \delta - \kappa = 0 \quad \vee\, Y = \delta + \kappa = 0. \tag{34}$$

At these turning points, one of the corrections in the potential (30) or (31) diverges. Thus, it is wise to solve the approximate equation (32) or (33) for that quantity where the correction to the potential is small even at the turning points.

To make the discussion more precise, we consider only the family of generic potentials with one or two classical turning points, to avoid internal resonances in the mirror. Such potentials are shown in Fig. 6. The potentials shown arise if we consider a chirped mirror that generates a negative GDD, the case we want to concentrate on in the following. The detailed parameters of the mirror will be discussed later. The potential is shown for two different wavelengths, 800 and 950 nm. As we can see, the long wavelength is reflected more deeply inside the mirror than the short wavelength, which leads to the negative dispersion.

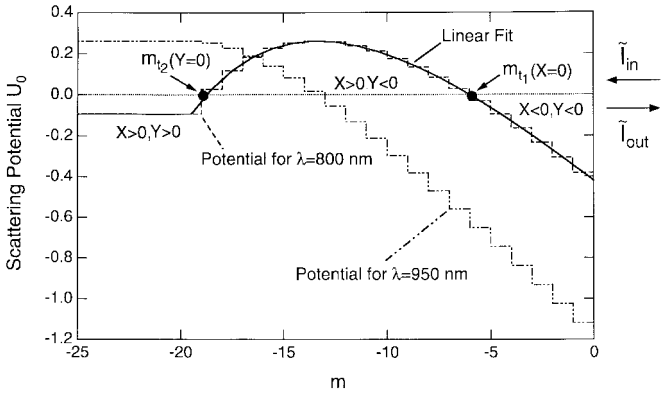

Fig. 6. Scattering potential U_0 for two different wavelengths of a chirped mirror consisting of 25 layer pairs, with $n_h = 2.5$ and $n_l = 1.5$. The Bragg wavenumber is linearly chirped from $k_0 = 2\pi/(600\text{ nm})$ to $k_{min} = 2\pi/(900\text{ nm})$ over the first 20 index steps and then kept constant. For numerical evaluation of the WKB-solution, the steps in the potential are linearly fitted.

From Fig. 4(a), we see that $\kappa < 0$ for $|\Delta\phi| \ll \pi$. For a chirped mirror with negative GDD, i.e., the Bragg wavenumber is decreasing with increasing $|m|$, for a fixed wavelength, the detuning is negative in the front section of the mirror and increases along the mirror due to the decrease in the Bragg wavenumber. Therefore, the right turning point m_{t_1} corresponds to the condition $X = 0$ and the left turning point m_{t_2} corresponds to $Y = 0$, see Fig. 6. As discussed before, the right turning point is a singularity in the scattering potential for the voltage according to (30) and the left turning point for the current according to (31). Thus, for a wave incident from the right, we can apply the WKB-method only to the Schrödinger equation for the current (33) and determine the corresponding voltage via (19), which is not singular anywhere in this range. For evaluation of the WKB-expressions, the scattering potential U_0 has to be a continuous function. Thus, for the numerical calculations, we fit two neighboring and piecewise constant parts of the scattering potential linearly, as shown in Fig. 6.

In Appendix A, we derive the standard WKB-solution for the range where $X < 0$ for a highly reflecting mirror. The result is

$$\tilde{I}(m) = \frac{1}{\sqrt{q(m)}}\,\sin\left(\phi_I(m)\right) \tag{35}$$

with

$$\phi_I(m) = \frac{\pi}{4} + \int_{m_{t_1}}^{m} q(\overline{m})\, d\overline{m} \tag{36}$$

where $m \in [m_{t_1}, 0]$. The frequency range of high reflectivity is the range of interest in mirror design. Here, q is the propagation constant, where the solution has an oscillatory behavior

$$q(m) = \sqrt{-U_0} = \sqrt{X\,Y} = \sqrt{\delta^2 - \kappa^2}. \tag{37}$$

Then, we obtain for the current

$$I(m) = \frac{\sqrt{Y}}{\sqrt{q}}\,\sin(\phi_I) = \sqrt{\frac{\text{sign}(Y)}{Z}}\,\sin(\phi_I) \tag{38}$$

where

$$Z(m)=\sqrt{\frac{X}{Y}}=\sqrt{\frac{\delta-\kappa}{\delta+\kappa}} \tag{39}$$

is the characteristic impedance of the inhomogeneous transmission line. From (19), we obtain for the voltage

$$\begin{aligned}V(m)&=\frac{i}{Y}\,\frac{dI}{dm}\\&=\frac{i}{\sqrt{\operatorname{sign}(Y)}}\left\{q\cos(\phi_I)+\frac{Z'}{2q\sqrt{Z}}\,\sin(\phi_I)\right\}.\end{aligned} \tag{40}$$

The solutions for the current and the voltage determine the reflection coefficient of the mirror for a wave incident from the right with respect to the point $m=0$ by

$$\begin{aligned}r_{\mathrm{M}}(k)&=\frac{\tilde{A}(0)}{\tilde{B}(0)}=\frac{A(0)}{B(0)}=\frac{V(0)+I(0)}{V(0)-I(0)}\\&=-\frac{1+ix(0)}{1-ix(0)}.\end{aligned} \tag{41}$$

Here, we introduced the normalized impedance x given by

$$x=Z\tan(\tilde{\phi}_I)+\frac{Z'}{2q}\quad\text{with}\quad\tilde{\phi}_I=\phi_I-\frac{\pi}{2}. \tag{42}$$

Note, that for the scattering potential, as illustrated in Fig. 6, $Y(0)<0$, and therefore $\operatorname{sign}(Y(0))=-1$. In the WKB-approximation, the phase of the reflected light follows from (41) to be

$$\phi_{r_{\mathrm{M}}}(k)=\pi+2\arctan(x(0)) \tag{43}$$

and, therefore, the group delay T_{g} of the chirped mirror is generally given by

$$\begin{aligned}T_{\mathrm{g}}(k)&=-\frac{\partial\phi_{r_{\mathrm{M}}}}{\partial\omega}=-\frac{\partial k}{\partial\omega}\,\frac{\partial\phi_{r_{\mathrm{M}}}}{\partial k}\\&=-\frac{1}{c}\,\frac{2}{1+x^2}\,\frac{\partial x}{\partial k}\bigg|_{m=0}\\&=-\frac{1}{c}\,\frac{2}{1+x^2}\left\{\frac{\partial Z}{\partial k}\,\tan(\tilde{\phi}_I)\right.\\&\quad\left.+\frac{Z}{\cos^2(\tilde{\phi}_I)}\,\frac{\partial\tilde{\phi}_I}{\partial k}+\frac{1}{2}\,\frac{\partial}{\partial k}\left(\frac{Z'}{2q}\right)\right\}\bigg|_{m=0}.\end{aligned} \tag{44}$$

An important point to note is that the typical singularity of the WKB-solution at the classical turning point does not exist for the amplitude reflectivity $r_{\mathrm{M}}(k)$, although the current and voltage itself diverge at this point, because of the factor $1/\sqrt{q(m)}$. However, as will be discussed in Section IV-C, this singularity occurs again in the group delay due to the derivative of Z and Z' with respect to the wavenumber. These singularities could be avoided by using the exact solutions to the Schrödinger equations, linearized near the classical turning points, which are the well-known Airy-functions [17]. However, this would be at the expense of transparency of the equations. Thus, we stay with the expression derived above for the group delay (44).

The expressions for phase and group delay show the origin of the oscillation in the group delay arising from a simple-chirped mirror. If the long wavelength penetrate deep into the mirror the phase of the corresponding current wave $\tilde{\phi}_I$ reaches a value of several times 2π. Thus, the trigonometric functions of the phase $\tilde{\phi}_I$ occurring in (44) lead to strong oscillations in the group delay, because the phase $\tilde{\phi}_I$ depends strongly on frequency.

In the high-reflectivity region, the power transmission coefficient of the chirped mirror is given by [17]

$$\begin{aligned}T(k)&=\exp\left(-2\int_{m_{\mathrm{t}_2}}^{m_{\mathrm{t}_1}}\sqrt{U_0(m)}\,dm\right)\\&=\exp\left(-2\int_{m_{\mathrm{t}_2}}^{m_{\mathrm{t}_1}}\sqrt{\kappa^2-\delta^2}\,dm\right)\\&=1-R(k).\end{aligned} \tag{45}$$

in WKB-approximation, where R denotes the reflectivity of the mirror.

B. WKB-Solutions for a Mirror with Matched Impedance

From (42) to (44), we find that the oscillations in the phase and group delay vanish, if the characteristic impedance $Z(m=0)$ is identical to one and its derivative with respect to m vanishes, $Z'(m=0)=0$, for all frequencies. This is only achieved if the coupling coefficient and its derivative vanish at the beginning of the mirror

$$Z(m=0)=1\quad\forall\delta\Rightarrow\kappa(m=0)=0 \tag{46}$$

$$Z'(m=0)=0\quad\forall\delta\Rightarrow\kappa'(m=0)=0. \tag{47}$$

The physical reason for these conditions is impedance matching to the homogeneous low-index layer, where the structure is so far embedded and where the characteristic impedance is one due to the lack of coupling. The second condition, that the derivative of the impedance should also vanish, means that the coupling coefficient should be increased as slowly as possible in order to avoid spurious reflections. Thus, we have to increase the coupling coefficient in m at least with a power greater than 1 in order to be ideally matched to the low-index material. Equation (5) for the exact coupling coefficient shows that the adiabatically increase corresponds to a chirp in the thickness of the high-index layer.

Hence, to avoid spurious reflections at the front structure of the mirror, we have to chirp the two independent parameters in our theory, i.e., the Bragg wavenumber for an increase of the high-reflectivity range and the coupling coefficient for the impedance matching. Because of the required chirping of both parameters, we call these mirrors DCM's. In the case of an impedance matched DCM, the expression for the phase (43) simplifies to

$$\begin{aligned}\phi_{r_{\mathrm{M}}}(k)&=\pi+2\tilde{\phi}_I(0)\\&=\frac{\pi}{2}+2\int_{m_{\mathrm{t}_1}(k)}^{0}q(m)\,dm.\end{aligned} \tag{48}$$

Thus, for the matched case, the phase of the amplitude reflectivity is just two times the phase of the equivalent current wave ϕ_I from the beginning of the mirror to the classical turning point m_{t_1} of the scattering potential. For the

group delay and the GDD we obtain the following simple expressions:

$$\begin{aligned} T_{\mathrm{g}}(k) &= -\frac{1}{c}\,\frac{\partial \phi_{r_{\mathrm{M}}}}{\partial k} \\ &= -\frac{2}{c}\,\frac{\partial \phi_I}{\partial k} \\ &= -\frac{2}{c}\,\frac{\partial}{\partial k}\int_{m_{\mathrm{t}_1}(k)}^{0} q(m)\,dm \\ &= -\frac{2}{c}\int_{m_{\mathrm{t}_1}(k)}^{0}\left(\frac{\partial}{\partial k}\,q(m)\right)dm \end{aligned} \tag{49}$$

$$\begin{aligned} D_2(k) &= -\frac{2}{c^2}\,\frac{\partial^2}{\partial k^2}\int_{m_{\mathrm{t}_1}(k)}^{0} q(m)\,dm \\ &= -\frac{2}{c^2}\left\{\int_{m_{\mathrm{t}_1}(k)}^{0}\left(\frac{\partial^2}{\partial k^2}\,q(m)\right)dm \right. \\ &\quad \left. -\left(\frac{\partial}{\partial k}\,q(m)\right)\Big|_{m=m_{\mathrm{t}_1}}\frac{\partial}{\partial k}\,m_{\mathrm{t}_1}(k)\right\}. \end{aligned} \tag{50}$$

One has to note that the classical turning point is a function of wavenumber. The last equality for the group delay and the GDD holds because the integrand vanishes at the classical turning point according to (34), i.e., $q(m_{\mathrm{t}_1}) = 0$.

C. Comparison of Exact and WKB Results

In this section, we show that the derived WKB-expressions for reflectivity and group delay are not only of qualitative value, but even allow for a quantitative predesign of a chirped Bragg structure with a desired high reflectivity and group delay. We compare exact results obtained by the transfer matrix method with our WKB-results from the preceding subsections for a linearly chirped dielectric mirror, in the case of a matched and not matched impedance, respectively. The WKB-results are obtained by using the exact coupling and detuning coefficients from Section II and linearly fitting the scattering potential as shown in Fig. 6. In this section, we always consider the reflection with respect to the first SiO_2 layer. However, we do not take into account the index jump to the air as the ambient medium.

Fig. 7(a) and (b) shows the reflectivity and group delay for a mirror consisting of 25 index steps, where we have used the constant refractive indices $n_{\mathrm{l}} = 1.5$ and $n_{\mathrm{h}} = 2.5$ ($r = 0.25$), which are close to the indices of the standard dielectric materials SiO_2 and TiO_2. Here, we neglect any frequency dependence of the refractive indices. We varied the Bragg wavenumber linearly over the first 20 index steps from $k_0 = 2\pi/(600\text{ nm})$ to $k_{\min} = 2\pi/(900\text{ nm})$, according to $k = k_0 - (|m| - 1)\cdot(k_0 - k_{\min})/19$. For the last 5 index steps the Bragg wavenumber is kept constant on its minimum value $k_{\min}$. In all figures, the wavenumber is normalized to the maximum Bragg wavenumber k_0 for the first index step. Thus, in principle, the mirror is easily scalable to any desired wavelength range. Here, we choose a range suitable for sub-10-fs pulse generation from a Ti:sapphire laser, see [18] and [19].

In Fig. 7(a), the dashed and dotted curves show results for the case in which the impedance at the front of the mirror is not matched, i.e., the coupling coefficient is nearly constant over the whole mirror and the optical thickness of each layer is a quarter of the Bragg wavelength corresponding to each index step ($\Delta\phi(k_B(m)) = 0$). As can be seen, the WKB-results fit very well to the exact results in the region where the resulting mirror is highly reflective, namely from about $k/k_0 = 0.59 - 1.03$ (580–1020 nm). Even the group delay shows an excellent agreement over the full high-reflectivity range, except for the range around 0.85. At this wavenumber, the right turning point coincides with the front of the mirror and the group delay of the WKB-solution diverges. This happens because the reactance X vanishes at the turning point and, therefore, the derivative of the impedance Z with respect to wavenumber in (44) leads to a singularity in the group delay. Obviously, the high-reflectivity range of the mirror already covers most of the fluorescence bandwidth of Ti:sapphire. However, the strong oscillations in the group delay, with amplitudes as large as ± 25 fs, prevent the use of such mirrors for ultrashort-pulse generation in the range of 50 fs or even shorter. These oscillations arise because longer wavelengths are reflected deep inside the mirror and they have to pass the Bragg stack responsible for reflecting the shorter wavelengths. The interference of the partial reflection at this stack, together with the strong reflection from the back of the mirror, leads to the formation of a GTI for the long wavelength. The result is a strong periodic oscillation of the group delay well known for a GTI.

As we have shown in the preceding subsection, if we additionally chirp the coupling coefficient from zero at the front of the mirror to its maximum value, we should be able to eliminate these oscillations and we should achieve a smooth group delay over the high-reflectivity wavelength range of the mirror. The solid and dash–dotted curves in Fig. 7(a) and (b) show the reflectivity and group delay for a DCM, where the Bragg wavenumber is chirped over the same wavelength range as before, but in addition, also the coupling coefficient is chirped separately over the first 12 index steps. This means that the Bragg wavelength, which is given by twice of the total optical thickness of the high- and low-index layer of each symmetrical index step, is again chirped from 600 to 900 nm, but the layers are far away from quarter-wave layers in the front section of the mirror, i.e., $\Delta\phi(k_B(m)) \neq 0$. We chirp the thickness of the high-index layer according to $d_{h,m} = \pi/(2k_B(12)n_h)\cdot(|m|/12)^{\alpha}$ over the first 12 index steps to achieve impedance matching. The solid line in Fig. 7(a) shows the reflectivity and group delay, if the thickness of the high-index layer is chirped linearly over the first 12 index steps, i.e. $\alpha = 1$, and therefore, $Z'(0) \neq 0$. Again, the agreement between the exact and the WKB-results is excellent, both in reflectivity and group delay. Of course, the new mirror shows a reduced reflectivity for normalized wavenumbers beyond 0.96 (below 625 nm), due to the reduced coupling coefficient at the beginning of the structure. Now, the mirror is almost completely transmissive for normalized wavenumbers at around 1.2 (500 nm), which is in our case an additional advantageous side effect of the double chirping, because, at that wavelength range the mirror should be transparent for the pump light of the Ti:sapphire laser.

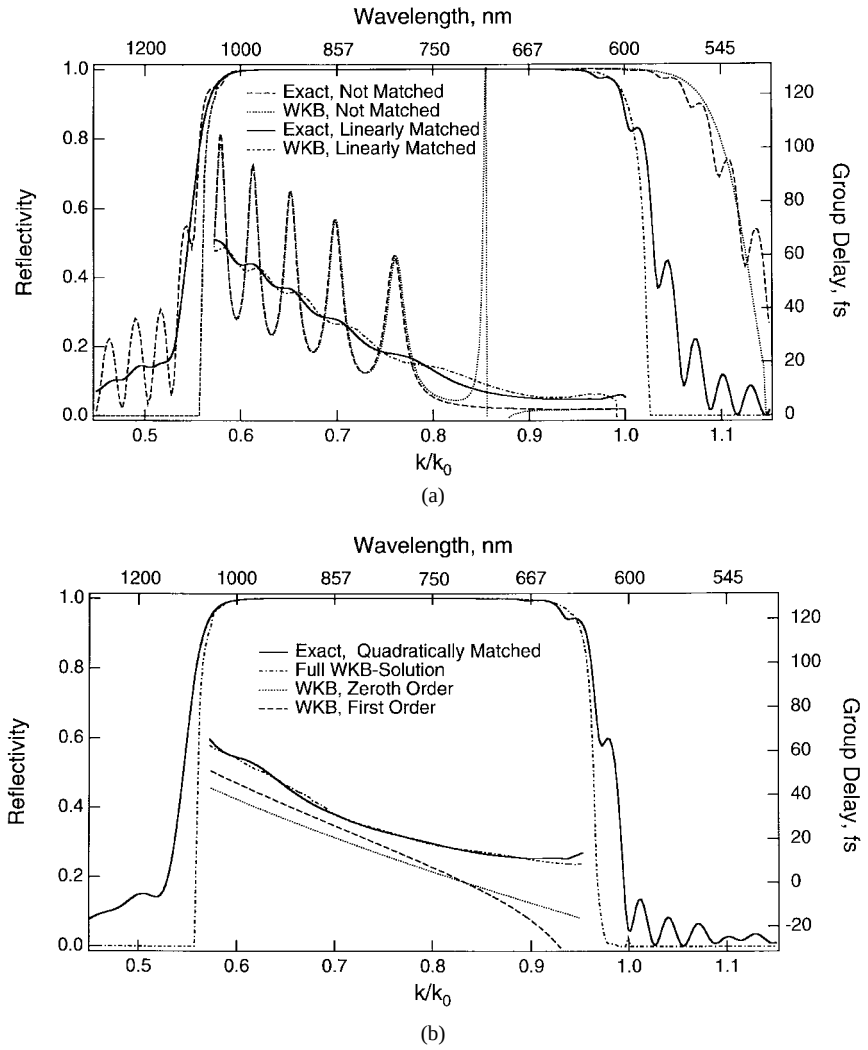

Fig. 7. Comparison of the exact reflectivity and group delay with the WKB-results for a mirror which is chirped in the Bragg wavenumber, as described in Fig. 6. (a) The dashed and the dotted lines show the results calculated with transfer matrix theory and the WKB-method, respectively. In these cases, the coupling coefficient is nearly constant for all wavelengths (i.e., impedance is not matched). This leads to a broad high-reflectivity range in combination with strong oscillations in the group delay. The solid and dash–dotted lines show the corresponding results if the thickness of the high-index layer is linearly chirped over the first 12 index steps. In that case, the oscillations are strongly reduced at the expense of the high-reflectivity range. (b) The solid and the dash–dotted lines show the exact and WKB-results, respectively, for a quadratically chirped thickness of the high-index layer. This results in a very smooth group delay. The figure also shows the group delay derived from an approximate expansion of the WKB-solution. The dotted line shows the zeroth-order approximation, and the dashed line shows the first-order approximation.

Note, the simple linear chirp already removed the undesired oscillations in the group delay considerably. Nevertheless, the oscillations are too strong for sub-10-fs pulse generation. Fig. 7(b) shows the result for a quadratically chirped coupling coefficient, i.e., $\alpha = 2$, and therefore, in addition $Z'(0) = 0$. However, this results in a very smooth group delay at the expense of an additional fraction of the high-reflectivity range.

In Section VI, we discuss practical limitations for the design of DCM's that prevent us from the direct use of mirrors as described in this section.

V. Application of the Theory on a DCM with a Linearly Chirped Bragg Wavenumber

The usefulness of the theory derived above can be further demonstrated by application to an example. We derive an analytic expression for the GDD of a DCM with a linearly chirped Bragg wavenumber. We show that a mirror with linear chirp always has the tendency to produce a positive third-order dispersion (TOD), which has already been found [20] but which has not yet been explained.

A. Analytic Expressions for the Dispersion of a Mirror

Generally, it is not possible to derive an analytic expression for the GDD, due to the complexity of the propagation constant $q(m) = \sqrt{\delta^2 - \kappa^2}$ in (50). However, to gain further insight into the dispersion that can be generated by a given mirror, we develop in this chapter approximate expressions for the dispersion of a linearly chirped mirror. Therefore, we expand the square root in a series according to

$$\sqrt{\delta^2 - \kappa^2} = |\delta| \sum_{\mu=0}^{\infty} \binom{1/2}{\mu} \left(-\frac{\kappa^2}{\delta^2}\right)^{\mu} \tag{51}$$

since $\delta^2 \geqq \kappa^2$ in the interval $[m_{t_1}, 0]$ and we take only

the zeroth-order term $|\delta|$ for an analytic computation of the phase properties. In Appendix B, we give the results for the first-order correction term which is quadratic in κ.

Now, we further simplify the coupling coefficient (14) from Section II by $\kappa(m) = \kappa_0 = -2r = \text{const}$. This additional approximation is justified if we assume that the impedance matching section of the mirror is short compared to the rest of the mirror. Then, most of the layers are near quarter-wave layers for all wavelengths and, therefore, $|\Delta\phi| \ll \pi$. As shown in Fig. 4, the simplified linear approximation for the detuning coefficient (15) around $\phi = \pi$ is always sufficient for arbitrary $\Delta\phi$, whereas the strong dependence of the exact coupling coefficient on $\Delta\phi$ will have a detrimental impact on the results. Later on in this section, we will see that deviations to the full WKB-solution are caused by the neglect of the higher order terms in the sum above and the assumption of a constant coupling coefficient. Nevertheless, the approach taken here gives analytical insight.

Thus, for the group delay (49) we obtain to lowest order with (15)

$$\begin{aligned} T_{\mathrm{g}}^0(k) &= -\frac{2}{c}\int_{m_{\mathrm{t}_1}(k)}^{0} \frac{\partial}{\partial k}\,|\delta|\,dm \\ &= \frac{2\pi}{c}\int_{m_{\mathrm{t}_1}(k)}^{0} \frac{1}{k_B(m)}\,dm \\ &= \frac{1}{c}\int_{m_{\mathrm{t}_1}(k)}^{0} \lambda_B(m)\,dm. \end{aligned} \tag{52}$$

As we can see, the group delay in zeroth-order approximation is given by the time delay of the light from the front of the mirror to the classical turning point and back.

The right turning point is implicitly defined by condition (34), which results in

$$k_B(m_{\mathrm{t}_1}(k)) = \frac{1}{1+\dfrac{\kappa_0}{\pi}}\,k \tag{53}$$

if the coupling coefficient is assumed to be constant. The linearly chirped Bragg wavenumber at the different positions in the mirror can be written as

$$k_B(m) = k_0 + k_1 m, \quad k_0, k_1 > 0, m \in [m_{\mathrm{t}_1}, 0]. \tag{54}$$

For this case, the classical turning point follows from (53) according to

$$m_{\mathrm{t}_1}(k) = \frac{k_0}{k_1}\left\{\frac{\pi}{\pi - |\kappa_0|}\,\frac{k}{k_0} - 1\right\}. \tag{55}$$

Hence, with (54) and (55), (52) yields for the group delay of a linearly chirped mirror to lowest order

$$\begin{aligned} T_{\mathrm{g}}^0(k) &= \frac{2\pi}{ck_1}\,\ln\left(\frac{\pi - |\kappa_0|}{\pi}\,\frac{k_0}{k}\right) \\ &= \frac{2\pi}{ck_1}\left\{\ln\left(1 - \frac{|\kappa_0|}{\pi}\right) + \ln\left(\frac{k_0}{k}\right)\right\}. \end{aligned} \tag{56}$$

Using this result, the GDD follows directly to

$$D_2^0(k) = -\frac{2\pi}{c^2 k_1 k_0}\left(\frac{k_0}{k}\right) \tag{57}$$

and finally, for the TOD we obtain

$$D_3^0(k) = \frac{2\pi}{c^3 k_1 k_0^2}\left(\frac{k_0}{k}\right)^2 > 0. \tag{58}$$

B. Discussion of Results

Equation (58) shows that a linearly chirped mirror has a positive TOD, although one might think that a linear chirp in the Bragg wavenumber would lead to a linear group delay, i.e., vanishing TOD. Obviously, in this case, only the classical turning point m_{t_1} depends linearly on the wavenumber k, but the GDD shows a hyperbolic dependence. If we take the values from the example discussed in detail in Section IV, ($\kappa_0 = -0.5$, $k_0 = 10.47\ \mu\mathrm{m}^{-1}$, $k_1 = 0.17\ \mu\mathrm{m}^{-1}$) the GDD can be written as

$$D_2^0(k) \approx -39\frac{k_0}{k}\ \mathrm{fs}^2 \tag{59}$$

and, for the TOD, we obtain

$$D_3^0(k) \approx 12\left(\frac{k_0}{k}\right)^2\ \mathrm{fs}^3. \tag{60}$$

From these expressions, for the dispersion at 800-nm wavelength, i.e., $k/k_0 = 0.75$, we estimate the following values: $D_2^0 \approx -52\ \mathrm{fs}^2$ and $D_3^0 \approx 21\ \mathrm{fs}^3$.

It is remarkable that, to lowest order, within our approximations, (57) and (58) do not depend on the coupling coefficient. The coupling coefficient itself only influences the group delay by an additive constant and, most importantly, the reflectivity of the mirror.

In Fig. 7(b), we plotted the zeroth-order approximation of the group delay, (56), and the first-order approximation, (B1), given in Appendix B, in addition to the exact group delay and the full WKB-solution. The agreement of the simplified zeroth- and first-order expressions with the exact results is remarkably good, and gives the right order of magnitude for the group delay. The deviations are due to the neglect of the higher order terms and the fact that the prerequisite of an almost constant coupling coefficient is not fulfilled in the example of Section IV. The reason is that for demonstration of the double-chirp technique the impedance was quadratically matched very slowly over the first 12 index steps. That is nearly half of the mirror and, therefore, the assumption of a short impedance matching section is not really satisfied. This leads to the stronger curvature of the exact group delay in comparison to the zeroth- and first-order approximation of the WKB-solution. Additionally, the explicit additive dependence of (56) on the coupling coefficient results in a critical dependence of the absolute group delay value. In contrast, the accuracy of the approximate GDD and TOD relative to the group delay is better due to their independence of the coupling coefficient. To summarize this section, although the expressions derived for this example are not very precise, they allow for an estimate of the desired dispersion properties of the mirror. Therefore, they can be used to compute a good starting structure for later computer optimization.

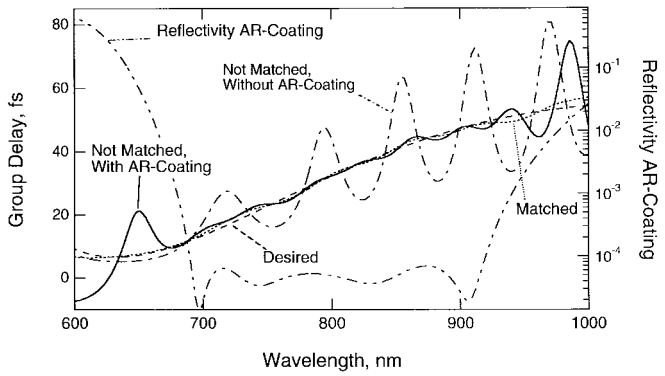

Fig. 8. Influence of the different design steps on the theoretical design of a chirped mirror. The dashed line shows the desired group delay for a particular design problem. The dotted line represents the group delay of the analytically predesigned mirror without an AR-coating but ideally matched to the ambient medium. The dash–dotted line indicates the group delay of the analytically predesigned mirror, not matched to the air. The solid line shows suppression of the oscillations when an AR-coating is put on top of the predesigned mirror. Also shown is the reflectivity of the 14-layer AR-coating.

VI. Design of a Broad-Band DCM

The design of a complete mirror is more complicated than that which has been discussed so far. Till now the reflectivity of the mirror was calculated with respect to a reference plane in the first low-index layer. The structure still has to be matched to air. The jump from air to the low-index material again introduces a reflection and, therefore, a GTI-like oscillation in the group delay, which makes the design useless, despite the impedance matching structure at the front part of the mirror. Note, that it is not possible to find an easy solution for the matching problem to air, as described by the adiabatic increase of the coupling coefficient. Therefore, we design a broad-band AR-coating in order to suppress oscillations caused by these additional GTI-like effects as much as possible.

Fig. 8 illustrates the influence of the different matching problems on the group delay by an example. The dashed line shows the desired group delay for a particular design problem. Assuming, that we are ideally matched to the ambient medium, we can design a mirror with a group delay, which follows closely the desired group delay (dotted line). This analytic design is nearly perfect over a wavelength range from 600 to 1000 nm. The bandwidth is limited due to the limited number of layers and small deviations are caused by the finite length of the thinnest layer. If we take the refractive-index jump from air to the first layer into account, that causes a reflection of about 4%, we end up with the dashed-dotted curve, where we clearly see strong oscillations. If we put a 14-layer AR-coating on top of the mirror, we obtain the solid curve. Obviously, the oscillations are only suppressed in the wavelength range from about 680–920 nm, in which the reflectivity of the AR-coating, ($-\cdot\cdot-\cdot\cdot-$ line), is low enough to suppress the GTI-effects sufficiently. Thus, our current limitation in the theoretical design of a DCM is given by the bandwidth of about 240 nm, over which we can easily achieve an AR-coating with a reflectivity less than 10^{-4}.

Nevertheless, the theoretical design (solid line) is an excellent approximation to the desired design goal. This analytic predesign can be used as a starting structure for a computer optimization program which improves the design performance, i.e., it minimizes the oscillations in the group delay and modifies the reflectivity slightly, if necessary. Our designs are optimized using a standard gradient method (Broyden–Fletcher–Goldfarb–Shanno algorithm from [21]), because we already start from a design that is close to the design goal.

As an example, Fig. 9 shows the desired and designed properties of a broad-band DCM after computer optimization, as well as the measured properties of the fabricated mirror. The desired group delay, Fig. 9(a), is exactly the group delay shown in Fig. 8. The final mirror consists of 62 layers and was designed to show the following properties: a reflectivity of more than 99.8% over a bandwidth of about 400 nm (620–1020 nm), a high transmission from 480 to 550 nm ($R < 3\%$) useful for different pump lasers (e.g. argon–ion laser around 500 nm, frequency-doubled Nd:Yag laser at 532 nm). The deviations in the group delay from the desired values are less than ± 1 fs in the high-reflectivity region [Fig. 9(a)]. Fig. 9(b) shows the resulting GDD. Obviously, the measured mirror properties are very close to the designed properties, although the dispersion characteristic is extremely sensitive on deposition errors. The precise fabrication of the mirrors is achieved by using ion beam sputtering [22] with an active layer control during growth [23].

Recently, similar DCM's with much smaller oscillations in the GDD, however, over a restricted wavelength range of about 250 nm have been used to generate pulses as short as 6.5 fs directly from the laser [18], [19]. In contrast, the current mirror design is appropriate for the tunability of $\approx$30 fs pulses from 700 to 1000 nm, which covers most of the full gain–bandwidth of Ti:sapphire. Additionally, the use of these DCM's allows for the generation of sub-10-fs pulses directly from the oscillator. However, the tradeoff between broad-band tunability and smoothness of the GDD prohibited the generation of pulses shorter than 8 fs [14]. The published broad-band mirrors show only reflectivities of more than 99.0% over a range of 400 nm and with considerably larger oscillations in the group delay. This allows only for tuning of 85-fs pulses over a bandwidth of less than 300 nm [24].

VII. Conclusion

We have presented an analytic treatment of chirped mirrors that is based on an exact coupled-mode theory and WKB-analysis. The transformation to a quantum mechanical scattering problem leads to a clear physical understanding of how a chirped mirror works and the related design problems. Explicit formulae for reflectivity and group delay have been derived from the WKB-solutions. A comparison with exact results obtained from the transfer matrix formalism shows that the WKB-results are rather accurate in the high-reflectivity region, which is the interesting range in the mirror design. The WKB-solutions explain the oscillations typically observed in the group delay as an impedance matching problem in the front section of the mirror and the air. Matching the impedance to the low-index layer is equivalent to an adiabatic increase of the coupling coefficient, that leads to the DCM design method. Application of the theory to a linearly chirped mirror

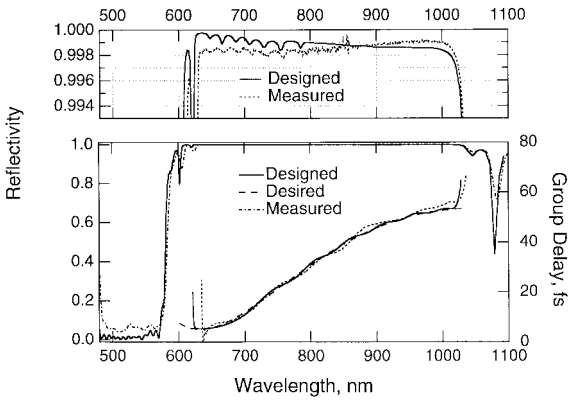

(a)

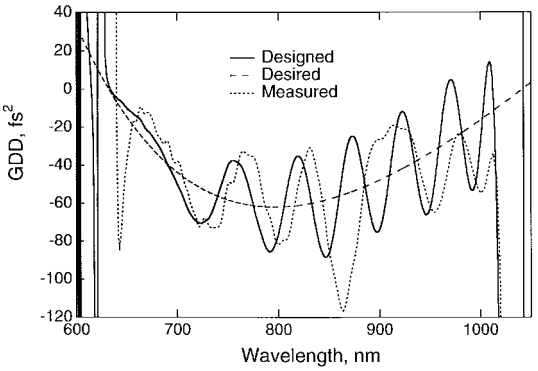

(b)

Fig. 9. Broad-band design of a DCM. (a) Designed and measured reflectivity and group delay. Also shown is the desired group delay. The bandwidth of the highly reflective region is about 400 nm for $R > 99.8\%$. The deviation of the designed to the desired group delay is less than 1 fs over the entire high-reflectivity range. (b) Designed, desired, and measured GDD of the mirror. The amplitude of the oscillations of the designed GDD is less than 25–30 fs^2 over the wavelength range from 620 to 1020 nm. As can be seen, the measured data of the DCM lie closely to the designed curves.

results in simple expressions for the GDD and TOD, that are useful for an estimation of the dispersion expected for given chirp parameters. This is only one example that illustrates the usefulness of the theory. Further investigations of the WKB-solutions derived in this paper should allow for an even better "straight forward" mirror design in the near future.

The major problem in the practical design of a DCM is the matching of the Bragg mirror to the ambient medium (air). Currently, we solve this problem by a broad-band AR-coating. This might not be the optimum solution to the matching problems involved in chirped mirror design. Thus, further investigations are necessary to find analytical solutions for the matching problems.

Finally, we have demonstrated the design of broad-band DCM's with a reflectivity of more than 99.8% and a smooth group delay over an extended bandwidth of about 400 nm.

APPENDIX A
DERIVATION OF THE SEMICLASSICAL WKB-SOLUTION

Here, we introduce an ordering parameter $\varepsilon \ll 1$ in order to derive the solution for the current $\tilde{I}$ as an asymptotic expansion with respect to this parameter. The condition of a slowly varying potential in the semiclassical limit is then equivalent to a rescaling of all derivatives in the Schrödinger equation (33) by $(d/dm) \to \varepsilon(d/dm)$ [25]. Thus, we obtain from (26) with (28) and (31):

$$-\varepsilon^2 \frac{d^2\tilde{I}}{dm^2} + (U_0 + \varepsilon^2 U_{I,1})\tilde{I} = 0. \tag{A1}$$

Now, we write the solution of this equation as an asymptotic expansion in ε [17], i.e.,

$$\tilde{I} = \exp\left(\frac{h_{-1}}{\varepsilon} + h_0 + \varepsilon h_1 + \cdots\right). \tag{A2}$$

For the three lowest order expansion coefficients h_{-1}, h_0 and h_1, after substitution of expansion (A2) into (A1), we obtain

$$\varepsilon^0\text{: } h_{-1} = \pm \int \sqrt{U_0}\, d\overline{m} \tag{A3}$$

$$\varepsilon^1\text{: } h_0 = -\frac{1}{4} \ln(U_0) \tag{A4}$$

$$\varepsilon^2\text{: } h_1 = \pm \int \frac{1}{2\sqrt{U_0}} \left\{U_{I,1} + \frac{U_0''}{4U_0} - \frac{5}{16}\frac{U_0'^2}{U_0^2}\right\} d\overline{m}. \tag{A5}$$

In solving the Schrödinger equation (A1), we assumed that the potential has the shape as shown in Fig. 6. We further assume that the reflectivity is high, so that we can neglect reflections from the left turning point m_{t_2}. Then, the semiclassical WKB-solution for this Schrödinger equation can be written as

$$\tilde{I}(m) = \frac{1}{\sqrt{q(m)}} \sin(\phi_I(m)) \tag{A6}$$

where q is an effective propagation constant and ϕ_I is the phase of the current wave from the beginning of the mirror to the classical turning point. Equation (A6) follows from (A2) with (A3)–(A5) and by asymptotically fitting the wave function on the left and right side of the right turning point m_{t_1} [17], for $\varepsilon = 1$,

$$q = \sqrt{-U_0} \geqq 0, \qquad \text{for } m \geqq m_{t_1} \tag{A7}$$

and

$$\phi_I(m) = \frac{\pi}{4} + \int_{m_{t_1}}^{m} q(\overline{m})\, d\overline{m} + \phi_2 \tag{A8}$$

with

$$\phi_2 = -\int_{m_{t_1}}^{m} \frac{1}{2q} \left\{U_{I,1} + \frac{1}{4}\frac{U_0''}{U_0} - \frac{5}{16}\frac{U_0'^2}{U_0^2}\right\} d\overline{m}. \tag{A9}$$

ϕ_2 is a second-order correction to the phase, which is one order beyond the standard WKB-solution. In the paper, we neglect this additional phase shift ϕ_2, which means that we consider only the zeroth-order term U_0 of the scattering potential.

APPENDIX B
FIRST-ORDER TERMS OF THE EXPANSION OF THE WKB-SOLUTION

With the first-order correction $-\kappa_0^2/(2|\delta|)$ of the propagation constant $q(m)$, the first-order contributions to the group delay and GDD are calculated in the same way as was demonstrated in Section V. The results are

$$T_{\mathrm{g}}^1(k) = -\frac{\kappa_0^2}{2}\int_{m_{t_1}}^{m} \frac{\partial}{\partial k}\,\frac{1}{|\delta|}\,dm$$
$$= \frac{\kappa_0^2}{\pi c k_1}\left\{\frac{\pi}{|\kappa_0|} - \left(1-\frac{k}{k_0}\right)^{-1} + \ln\left[\left(\frac{\pi}{|\kappa_0|}-1\right)\left(\frac{k_0}{k}-1\right)\right]\right\} \quad \text{(B1)}$$

$$D_2^1(k) = -\frac{\kappa_0^2}{\pi c^2 k_1 k_0}\,\frac{k_0}{k}\left(1-\frac{k}{k_0}\right)^{-2}. \quad \text{(B2)}$$

Thus, the complete group delay and GDD, up to first order, are given by $T_{\mathrm{g}}^0 + T_{\mathrm{g}}^1$ and $D_2^0 + D_2^1$, with T_{g}^0 and D_2^0 given in Section V.

ACKNOWLEDGMENT

F. X. Kärtner acknowledges helpful discussions with Prof. H. A. Haus. The authors greatly appreciate the fabrication of the DCM's at the Technische Hochschule Darmstadt by Dr. V. Scheuer and Prof. T. Tschudi. They are also grateful to Dr. I. D. Jung and D. H. Sutter for measuring the reflectivity and dispersion of the DCM's.

REFERENCES

[1] S. De Silvestri, P. Laporta, and O. Svelto, "Analysis of quarter-wave dielectric-mirror dispersion in femtosecond dye-laser cavities," *Opt. Lett.*, vol. 9, pp. 335–337, 1984.
[2] P. Laporta and V. Magni, "Dispersive effects in the reflection of femtosecond optical pulses from broadband dielectric mirrors," *Appl. Opt.*, vol. 24, pp. 2014–2020, 1985.
[3] R. Szipöcs, K. Ferencz, C. Spielmann, and F. Krausz, "Chirped multilayer coatings for broadband dispersion control in femtosecond lasers," *Opt. Lett.*, vol. 19, pp. 201–203, 1994.
[4] R. Szipöcs, A. Stingl, C. Spielmann, and F. Krausz, "Chirped dielectric mirrors for dispersion control in femtosecond laser systems," in *SPIE*, 1995, vol. 2377, pp. 11–22.
[5] A. Stingl, M. Lenzner, Ch. Spielmann, F. Krausz, and R. Szipöcs, "Sub-10 fs mirror-dispersion-controlled Ti:sapphire laser," *Opt. Lett.*, vol. 20, pp. 602–604, 1995.
[6] M. T. Asaki, C.-P. Huang, D. Garvey, J. Zhou, H. C. Kapteyn, and M. N. Murnane, "Generation of 11 fs pulses from a self-mode-locked Ti:sapphire laser," *Opt. Lett.*, vol. 18, pp. 977–979, 1993.
[7] S. De Silvestri, private communication, 1997.
[8] F. Gires and P. Tournois, "Interferometre utilisable pour la compression d'impulsions lumineuses modulees en frequence," *C. R. Acad. Sci. Paris*, vol. 258, pp. 6112–6115, 1964.
[9] G. Tempea, F. Krausz, K. Ferencz, and Ch. Spielmann, "Advances in chirped mirror technology," presented at the Conf. Ultrafast Optics, Monterey, CA, Aug. 3–8, 1997, paper TP-12.
[10] F. Ouellette, "Dispersion cancellation using linearly chirped Bragg grating filters in optical waveguides," *Opt. Lett.*, vol. 12, pp. 847–849, 1987.
[11] P. Tournois and P. Hartemann, "Bulk chirped Bragg reflectors for light pulse compression and expansion," *Opt. Commun.*, vol. 119, pp. 569–575, 1995.
[12] N. Matuschek, F. X. Kärtner, and U. Keller, "Exact coupled-mode theories for multilayer interference coatings with arbitrary strong index modulations," *IEEE J. Quantum Electron.*, vol. 33, pp. 295–302, 1997.
[13] F. X. Kärtner, N. Matuschek, T. Schibli, U. Keller, H. A. Haus, C. Heine, R. Morf, V. Scheuer, M. Tilsch, and T. Tschudi, "Design and fabrication of double-chirped mirrors," *Opt. Lett.*, vol. 22, pp. 831–833, 1997.
[14] D. H. Sutter, I. D. Jung, N. Matuschek, F. Morier-Genoud, F. X. Kärtner, and U. Keller, "300 nm tunability of 30-fs Ti:sapphire laser pulses with a single set of double-chirped mirrors," presented at the Conference on Lasers and Electrooptics (CLEO '98), San Francisco, CA, May 3–8, 1998, paper CThC5.
[15] R. E. Collin, *Foundations of Microwave Engineering*. New York: McGraw-Hill, 1992.
[16] J. R. Pierce, *Almost All about Waves*. Cambridge, MA: MIT Press, 1974.
[17] A. B. Migdal, *Qualitative Methods in Quantum Theory*. New York: Addison-Wesley, 1977.
[18] I. D. Jung, F. X. Kärtner, N. Matuschek, D. H. Sutter, F. Morier-Genoud, U. Keller, V. Scheuer, M. Tilsch, and T. Tschudi, "Self-starting 6.5 fs pulses from a KLM Ti:sapphire laser," *Opt. Lett.*, vol. 22, pp. 1009–1011, 1997.
[19] D. H. Sutter, I. D. Jung, N. Matuschek, F. Morier-Genoud, F. X. Kärtner, V. Scheuer, M. Tilsch, and T. Tschudi, and U. Keller, "Self-starting 6.5 fs pulses from a KLM Ti:sapphire laser using semiconductor saturable absorber and double-chirped mirrors," this issue, pp. 169–178.
[20] R. Szipöcs, and A. Kohazi-Kis, "Theory and design of chirped dielectric laser mirrors," *Appl. Phys. B*, vol. 65, pp. 115–135, 1997.
[21] W. H. Press, S. V. Teukolsky, W. T. Vetterling, and B. P. Flannery, *Numerical Recipes in Fortran*, 2nd ed. Cambridge, U.K.: Cambridge Univ. Press, 1994.
[22] V. Scheuer, M. Tilsch, and T. Tschudi, "Reduction of absorption losses in ion beam sputter deposition of optical coatings for the visible and near infrared," in *Conf. Proc. SPIE*, 1994, vol. 2253, pp. 445–454.
[23] M. Tilsch, V. Scheuer, and T. Tschudi, "Direct optical monitoring instrument with a double detection system for the control of multilayer systems from the visible to the near infrared," *Conf. Proc. SPIE*, 1994, vol. 2253, pp. 414–422.
[24] E. J. Mayer, J. Möbius, A. Euteneuer, W. W. Rühle, and R. Szipöcs, "Ultrabroadband chirped mirrors for femtosecond lasers," *Opt. Lett.*, vol. 22, pp. 528–530, 1997.
[25] Z. V. Lewis,"Semiclassical solutions of the Zakharov–Shabat scattering problem for phase modulated potentials," *Phys. Lett.*, vol. 112 A, no. 3, 4, pp. 99–103, 1985.

Nicolai Matuschek, for photograph and biography, see this issue, p. 178.

Franz X. Kärtner, for photograph and biography, see this issue, p. 168.

Ursula Keller (M'89), for photograph and biography, see this issue, p. 168.